

Dynamics of quantum observables and Born's rule in Bohmian Quantum Mechanics

Athanasios C. Tzemos* and George Contopoulos
Research Center for Astronomy and Applied Mathematics
of the Academy of Athens
Soranou Efessiou 4, GR-11527 Athens, Greece

Abstract

We investigate both ordered and chaotic Bohmian trajectories within the Born distribution of Bohmian particles of an anisotropic 2d quantum harmonic oscillator. We compute the average values of energy, momentum, angular momentum, and position using both Standard Quantum Mechanics and Bohmian Mechanics. In particular, we examine realizations of the Born distribution for a wavefunction with a single nodal point and two different wavefunctions with multiple nodal points: one with an almost equal number of ordered and chaotic trajectories, and another composed primarily of chaotic trajectories. Throughout our analysis, we focus on elucidating the contribution of ordered and chaotic Bohmian trajectories in determining these average values.

Introduction

Bohmian Quantum Mechanics (BQM) is a basic alternative interpretation of Quantum Mechanics [1, 2, 3, 4, 5]. In BQM the quantum particles follow deterministic trajectories, which are guided by the wavefunction describing the system, i.e. the solution of the Schrödinger equation:

$$-\frac{\hbar^2}{2M_q}\nabla^2\Psi + V\Psi = i\hbar\frac{\partial\Psi}{\partial t}, \quad q = x, y, \dots \quad (1)$$

according to the so called “Bohmian equations of motion”:

$$M_q\frac{dr}{dt} = \hbar\Im\left(\frac{\nabla\Psi}{\Psi}\right). \quad (2)$$

Thus the state of a quantum system in BQM is described by its wavefunction and the positions of the associated Bohmian particles in the configuration space.

BQM predicts the same experimental results as Standard Quantum Mechanics (SQM), when the Bohmian particles are distributed according to Born's rule (BR), which states that the probability density of finding a quantum particle in a certain region of space is equal

*atzemos@academyofathens.gr

to $P = |\Psi|^2$. If BR is initially satisfied then it is easily proved that it will be satisfied for all times. However, in BQM we are allowed to consider initial configurations of Bohmian particles distributed with $P_0 \neq |\Psi_0|^2$. Whether BR will be accessible in the long run in such cases is a fundamental problem in BQM and it has been shown that it depends strongly on the complexity of the Bohmian trajectories [6, 7, 8].

Chaos in Quantum Mechanics is an open field of research in the last decades and has attracted the interest of many authors. In Classical Mechanics we have a well understood definition of chaos: A nonlinear dynamical system is chaotic when it has a bound phase space and exhibits high sensitivity on small changes of its initial conditions. However, Standard Quantum Mechanics [9, 10, 11], does not predict trajectories for the quantum particles (due to the existence of Heisenberg's uncertainty). Moreover, the evolution of the wavefunction is described by Schrödinger's equation, i.e. a linear equation. Thus the notion of quantum chaos is not clearly defined in SQM and the majority of works in the field are focused on the comparison between the properties of quantum systems whose classical counterparts are ordered or chaotic [12, 13, 14, 15].

In contrast with SQM, BQM is a highly nonlinear trajectory-based quantum theory which allows the coexistence of ordered and chaotic Bohmian trajectories for a given quantum system. Thus it allows the study of chaotic dynamics in the quantum framework by use of all the techniques of the theory of classical dynamical systems, something that has been the main topic of many works [16, 17, 18, 19, 20, 21, 22, 23, 24, 25, 26, 27, 28, 29, 30].

In our series of works on Bohmian chaos we showed that the nodal points of the wavefunction Ψ (i.e. the points where $\Psi = 0$) are essential for the production of chaos. In fact, in the frame of reference of a moving nodal point N there is an unstable fixed point, the 'X-point'. Together they form the so called 'nodal point-X-point complexes' (NPXPC) which are characteristic geometrical structures of the Bohmian flow in the close neighbourhood of a nodal point. When a Bohmian particle comes close to an NPXPC it gets deflected by the X-point [31]. The effect of many such encounters is the emergence of chaos. Furthermore, in a recent paper [32] we showed that there are also unstable points in the inertial frame of reference, the 'Y-points' that play some role in the generation of chaos. Trajectories that never approach X-points or Y-points are in general ordered.

The study of the mechanism responsible for chaos production was crucial for understanding the role of order and chaos in the accessibility of BR by arbitrary initial distributions of Bohmian particles. In [33, 34] we emphasized the fact that any realization of the BR distribution made out of a finite number of Bohmian particles contains initial conditions that lead, in general, partly to chaotic and partly to ordered trajectories. Moreover, the chaotic trajectories of the systems that we studied were found to have a common footprint on the configuration space, i.e. their points acquire a common long time distribution regardless of their initial condition. We called this feature 'ergodicity' (this definition is different from the standard notion of ergodicity based on the metric transitivity in phase space). Thus the chaotic trajectories are ergodic (or partially ergodic, when the chaotic trajectories are divided into sets with different long time distributions [32]).

On the the other hand, the corresponding long time distributions of points of ordered trajectories cover limited regions of the configuration space. Thus we found that BR will be accessible only by initial distributions with the correct proportion between ordered and chaotic trajectories, and the correct distribution of ordered trajectories. It is also remarkable that the number of ordered trajectories in the BR distribution may not be negligible even in the case

of systems with multiple nodal points. Consequently, the common belief that a large number of nodal points guarantees the accessibility of Born's rule is in general not valid.

After all the above studies in the dynamics of Bohmian trajectories, it is reasonable for one to ask what is the role of the ordered and chaotic trajectories in deriving the same average values of observables as SQM, when $P_0 = |\Psi_0|^2$. This is the subject of the present paper, where we consider a number of 2d wavefunctions and we calculate the average values of the energy E , the momentum (p_x, p_y) , the angular momentum L and the position (x, y) of a large number of Bohmian particles, sampled according to the Born distribution. These values are compared with the corresponding values predicted by Standard Quantum Mechanics. By counting the numbers of ordered and chaotic trajectories in the Born distribution of these wavefunctions we examine their contribution in the average values.

Most works in the field of Bohmian chaos concentrate on non-interacting bound systems such as harmonic oscillators, with only a few addressing interacting systems like the quantum Henon-Heiles system [17, 35]. In the present paper, we consider again a simple quantum system which is classically integrable, that of an anisotropic 2d harmonic oscillator $V = \frac{1}{2}(\omega_x^2 x^2 + \omega_y^2 y^2)$. In this case the solutions of the Schrödinger equation are known analytically and the values of the various quantities can be calculated analytically as well. Details of these calculations are given in the Appendix. Moreover, the energy eigenstates of this system form a complete basis of Hilbert's space, i.e. any 2d wavefunction can be written as a linear combination of them. Consequently our results are not limited qualitatively in this special system.

We consider various wavefunctions which are superpositions of 3 energy eigenstates of the 2d oscillator. In particular, we study a case with a single nodal point (Section 2) and two cases with many nodal points (Section 3), one with equal proportions of ordered and chaotic trajectories and one example where chaotic trajectories dominate the BR distribution. In Section 4 we make our summary and comment on our results.

Wavefunction with a single node

We consider first a wavefunction with a single nodal point:

$$\Psi = M(a\Psi_{0,0} + b\Psi_{1,0} + c\Psi_{1,1}). \quad (3)$$

where $\Psi_{m,n}(x, y) = \Psi_m(x)\Psi_n(y)$. $\Psi_m(x)$ and $\Psi_n(y)$ are the 1-D energy eigenstates of the oscillator in x and y coordinates correspondingly, i.e.

$$\Psi_{m,n} = \prod_{q=x}^y N_q \exp\left(-\frac{\omega_q q^2}{2\hbar}\right) \exp\left(-\frac{i}{\hbar}E_s t\right) H_s\left(\sqrt{\frac{M_q \omega_q}{\hbar}}q\right), \quad (4)$$

where $s = m, n$ (integers) for $q = x$ and $q = y$ respectively and the normalization constant is $N_q = \frac{1}{\sqrt{2^s s!}} \left(\frac{M_q \omega_q}{\pi \hbar}\right)^{\frac{1}{4}}$. The functions H_m, H_n are Hermite polynomials in $\sqrt{\frac{M_x \omega_x}{\hbar}}x$ and $\sqrt{\frac{M_y \omega_y}{\hbar}}y$ of degrees m and n respectively and $E_s = (s + \frac{1}{2}) \hbar \omega_q$.

In this case there is only one nodal point (the equations $\Psi_R = \Psi_{Im} = 0$ are of first degree in x and y). In Fig. 1 we show a realization of the Born distribution $P = |\Psi|^2$ made out of

5000 particles, when $M_x = M_y = 1, \hbar = 1, a = b = 1, c = \sqrt{2}/2, \omega_x = 1, \omega_y = \sqrt{2}/2$. The value of the normalizing constant M is found by setting $M^2(a^2 + b^2 + c^2) = 1$. It is $M = \sqrt{2/5}$ ¹.

The red points represent the initial conditions which produce ordered trajectories and the blue points the initial conditions of chaotic trajectories.² We observe that the ordered trajectories dominate the BR distribution (almost 97%). The chaotic trajectories (3%) start in regions of small $P = |\Psi|^2$ at the boundaries of the two blobs as shown in the plane (x, y) (Fig. 1b).

The maximum value of P in the main blob is $P \simeq 0.33$ and in the secondary blob it is $P \simeq 0.06$. In Fig. 1c we give with colors the density of the points of the trajectories at every $\Delta t = 0.05$ of the BR distribution in a quadratic grid of bins up to a certain time t . Here we show the initial form of the colorplot at $t = 0$. It is clear that the maxima correspond to the tops of the two blobs while P decreases outwards.

Then we calculate the average value of the energy, according to SQM, which is [11]

$$\langle E \rangle = M^2(|a|^2 E_{0,0} + |b|^2 E_{1,0} + |c|^2 E_{1,1}), \quad (5)$$

where

$$E_{m,n} = (m + 1/2)\hbar\omega_x + (n + 1/2)\hbar\omega_y. \quad (6)$$

We remind that since $\Psi_{m,n}$ are eigenstates of the quantum harmonic oscillator (i.e. stationary states) $\langle E \rangle$ is constant in time. In the present case we find $\langle E \rangle = 1.595$.

On the other hand, the average values of the energy E_{av} of the Bohmian particles depend on their sampling in the realization of the Born distribution. Each particle has a total energy

$$E = K + V + Q, \quad (7)$$

where K is the kinetic energy $\frac{1}{2}(\dot{x}^2 + \dot{y}^2)$, V is the potential energy $V = \frac{1}{2}(\omega_x^2 x^2 + \omega_y^2 y^2)$ and Q is the Bohmian quantum potential energy $Q = -\frac{1}{2} \frac{\nabla^2 |\Psi|}{|\Psi|}$ which is time dependent and thus E is time dependent as well.

In Figs. 2a,b. we show typical examples of Bohmian trajectories, one chaotic and one ordered. We observe the complex shape of the chaotic trajectory and the close to Lissajous figure shape of the ordered trajectory, which covers a small region in the configuration space.

In Fig. 3 we take the average value E_{av} of the energy for various numbers of particles $N = 100, 200, \dots, 13000$ of a realization of the BR distribution at $t = 0$. These values show significant deviations from the analytical one for small numbers of Bohmian particles but for $N > 5000$ they tend to approach it.

For $N = 5000$ the average value is close to $E_{av} = 1.595$. But, in order to have a better estimation of E_{av} we have considered 5 different (random) realizations of the BR distribution with $N = 5000$ Bohmian particles. Their average value at $t = 0$ is $E_{av}(0) = 1.599 \pm 0.004$, i.e. it is a little above $\langle E \rangle$. If we integrate the trajectories of all realizations up to $t = 1000$ then

¹Although the wavefunction is defined from $-\infty$ to $+\infty$ in x and y the probability density $P = |\Psi|^2$ takes appreciable values for all times in the central region of space around the origin. In the present paper we work in regions of space where where $P > 10^{-5}$ for all times.

²We integrated for large times of order 10^5 the 5000 initial conditions of the BR distribution and counted which of them cover a large part of the configuration space. The corresponding trajectories were characterized as chaotic. On the other hand the trajectories whose form was that of a deformed Lissajous figure covering a small region in space were characterized as ordered. This practical algorithm which is based on the long time form of the Bohmian trajectories, ordered and chaotic, was introduced and extensively used in our previous works (see for example [32, 34]).

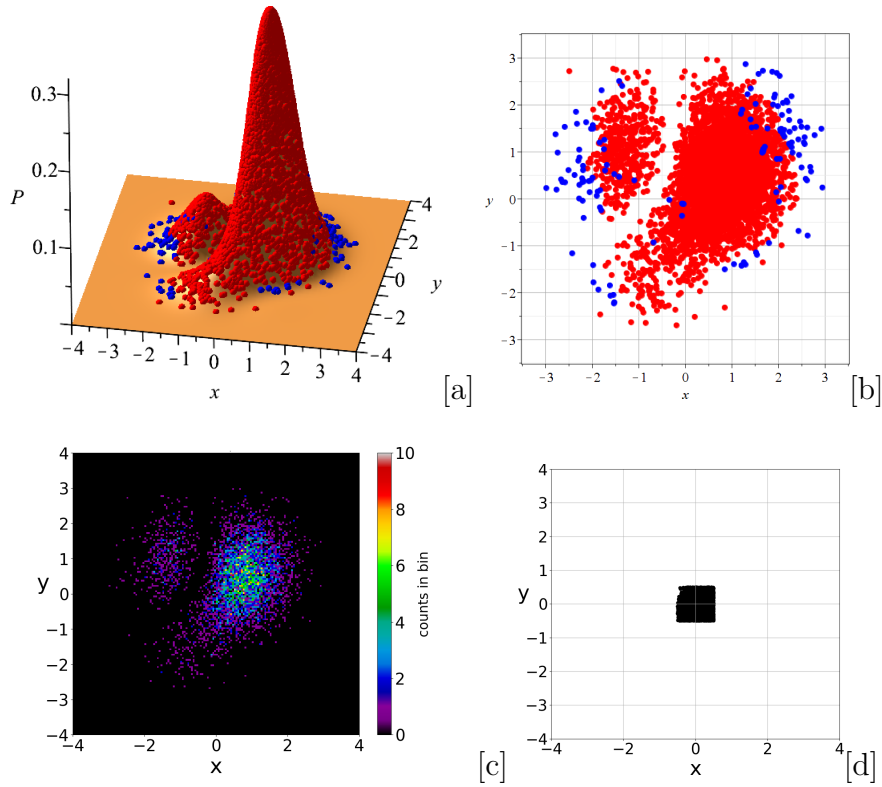


Figure 1: a,b,c: 5000 initial conditions of ordered (red) and chaotic (blue) trajectories distributed according to BR in the case of the wavefunction with a single nodal point: a) on the surface of $|\Psi|^2$ and b) on the $x - y$ plane. In c) we see their colorplot at $t = 0$. d) 5000 non-Born distributed initial conditions.

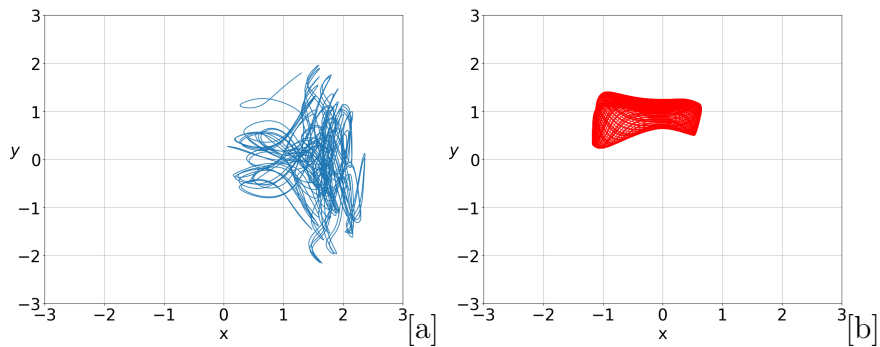


Figure 2: A chaotic trajectory ($x(0) = 1.3, y(0) = 1.8$) (a) and an ordered trajectory ($x(0) = 0.2, y(0) = 1.0$) (b) in the case of the single node wavefunction.

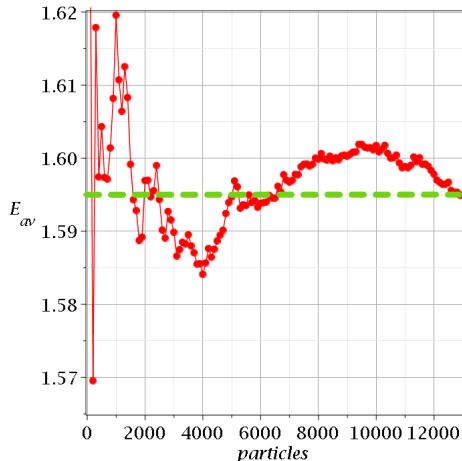


Figure 3: The average value of energy E_{av} at $t = 0$ as a function of the number of particles in a realization of Born's distribution for the wavefunction with a single nodal point.

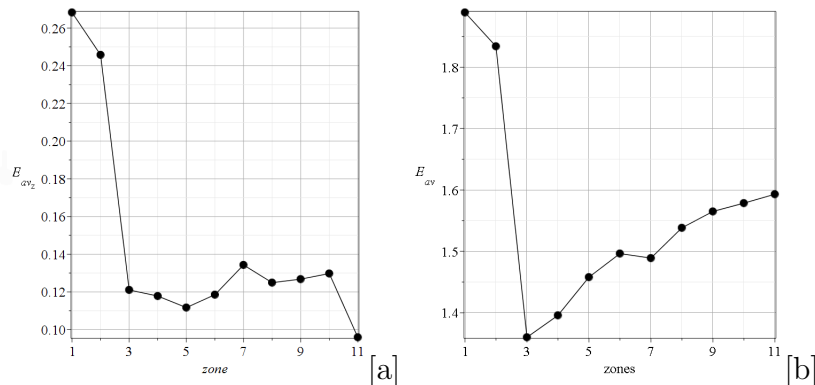


Figure 4: (a) The contributions of Bohmian particles in the successive zones (1 – 11) to the value of E_{av} at $t = 0$ (b) The separate values of E_{av} in the various zones.

we find that the mean absolute deviation between the analytical and the numerical values is ~ 0.005 , i.e. we can write $E_{av} = \langle E \rangle \pm 0.005$. Thus E_{av} has deviation from $\langle E \rangle = 1.595$ of order about 3%. By taking larger numbers of particles we find a better approach to $\langle E \rangle$, as expected.

On the other hand, in initial distributions of particles different from Born's rule we find quite different values of E_{av} . In a particular case with $P_0 \neq |\Psi_0|^2$ (Fig. 1d) we found $E_{av} = 0.819$, a value much smaller than $\langle E \rangle = 1.595$.

Then we separated the initial Born distribution of Fig. 1 into various zones of extent $\Delta P = 0.03$. Namely, the zones 1,2,...11 contain the particles with P in the intervals $0 < P < 0.03$, $0.03 < P < 0.06$, ... up to $0.3 < P < 0.33$. We calculated the contribution of the various zones in finding E_{av} and in Fig. 4a we give E_{av_z} , i.e. the energy of the particles in every zone divided by the total number $N = 5000$ of particles. We see that the zones 3,4,..10 contribute roughly equal amounts in E_{av} namely 0.123 ± 0.015 . The last zone (11) contributes a little less (0.096) and the two first zones contribute about double the average (0.268 in zone 1 and 0.246 in zone 2). In these two zones the contribution of the particles of the second blob is manifest.

If we take the average energy E_{av} in the various zones 1, 2, ... 11 by dividing their contribution by the corresponding number of particles (and not by 5000) we see that the average

value of the last zone is 1.593, very close to the global average (Fig. 4b). The previous zones (10, 9, ... 3) have decreasing values of E_{av} except for the first two zones (2 and 1) which have very large values because of the second blob.

On the other hand, the chaotic trajectories are very close to the bottom of the distribution ($P = 0$) and their average values of E_{av} is 1.38, smaller than the analytical value and close to the minimum value of Fig. 4b. It is notable that the chaotic trajectories do not give average values close to the analytical value. On the contrary the best approach is provided by the ordered trajectories on the top of the large blob of Fig. 1a. Therefore the claim that the distribution of particles tends to the Born distribution because of the chaotic trajectories is not valid in the present case, first because the number of the chaotic trajectories is small and second because the chaotic trajectories in the present case do not give the correct average value of the energy. Namely, if we start with an initial distribution of only chaotic trajectories we do not reach the Born distribution in the long run. In fact, even if we keep the correct proportions of ordered/chaotic trajectories, we cannot reach the Born distribution unless the ordered trajectories have the distribution found within the Born rule. E.g. if we take initially ordered trajectories only from the top of the large blob we will not ever reach the Born distribution.

Besides the values of the energy it is of interest to find the average values of other basic quantum observables as well, such as the momentum, angular momentum and position.

The average value of the p_x component of the momentum is given analytically by

$$\langle p_x \rangle = \int_{-\infty}^{\infty} \int_{-\infty}^{\infty} \Psi^* \hat{p}_x \Psi dx dy, \quad (8)$$

where $\hat{p}_x = -i\hbar \frac{\partial}{\partial x}$ is the corresponding momentum operator and Ψ^* is the complex conjugate of Ψ . The analytical calculation of $\langle p_x \rangle$ is given in the Appendix. There we show the various terms of the function $\Psi^* \hat{p}_x \Psi$ and indicate those terms that give nonzero contributions in the integral (8). In the present case we find after some algebra that

$$\langle p_x \rangle = -\frac{\sqrt{2\omega_x} ab \sin(\omega_x t)}{a^2 + b^2 + c^2}. \quad (9)$$

and similarly

$$\langle p_y \rangle = -\frac{\sqrt{2\omega_y} bc \sin(\omega_y t)}{a^2 + b^2 + c^2}. \quad (10)$$

Therefore $\langle p_x \rangle$ and $\langle p_y \rangle$ are time periodic with periods 2π and $2\pi\sqrt{2}$ respectively. In Fig. 5a we give the values of $\langle p_x \rangle$, which change with a period $T = 2\pi$, up to $t = 1000$. We have marked with red dots the values of $\langle p_x \rangle$ at every multiple of $t = 50$. In every interval $\Delta t = 50$ take place about 8 oscillations. If we calculate now the average values of $\langle p_x \rangle_{av}$ of 5000 particles at these times we find almost exactly the same values (blue dots) with a mean deviation in p_x equal to ~ 0.005 , i.e. of order 1%. Similar values are found in Fig. 5b for $\langle p_y \rangle$. The mean deviation in p_y is ~ 0.003 .

The average angular momentum is given analytically by

$$\begin{aligned} \langle L \rangle &= \int_{-\infty}^{\infty} \int_{-\infty}^{\infty} (\Psi^* x \hat{p}_y - y \hat{p}_x) \Psi dx dy \\ &= \frac{1}{\sqrt{\omega_x \omega_y}} \frac{ac(\omega_x - \omega_y) \sin((\omega_x + \omega_y)t)}{a^2 + b^2 + c^2} \end{aligned} \quad (11)$$

and similarly the average values $\langle x \rangle, \langle y \rangle$ are found equal to (see the Appendix for details):

$$\langle x \rangle = \sqrt{\frac{2}{\omega_x}} \frac{ab \cos(\omega_x t)}{a^2 + b^2 + c^2} \quad (12)$$

$$\langle y \rangle = \sqrt{\frac{2}{\omega_y}} \frac{ab \cos(\omega_y t)}{a^2 + b^2 + c^2}. \quad (13)$$

We note that

$$\langle p_x \rangle = \frac{d\langle x \rangle}{dt}, \quad \langle p_y \rangle = \frac{d\langle y \rangle}{dt}. \quad (14)$$

In the present case for $t = 0$ we have $\langle x \rangle = 0.566$ and $\langle y \rangle = 0.336$ while $\langle p_x(0) \rangle = \langle p_y(0) \rangle = 0$. The mean deviations between the values from SQM and the numerical values from our Bohmian simulation of $\langle L \rangle, \langle x \rangle, \langle y \rangle$ for $t \in [0, 1000]$ are very small (see Tab. 1).

For any arbitrary distribution of particles $P_0 \neq |\Psi_0|^2$ the mean deviations of the numerical average values from the analytical ones are in general large (see Table 1).

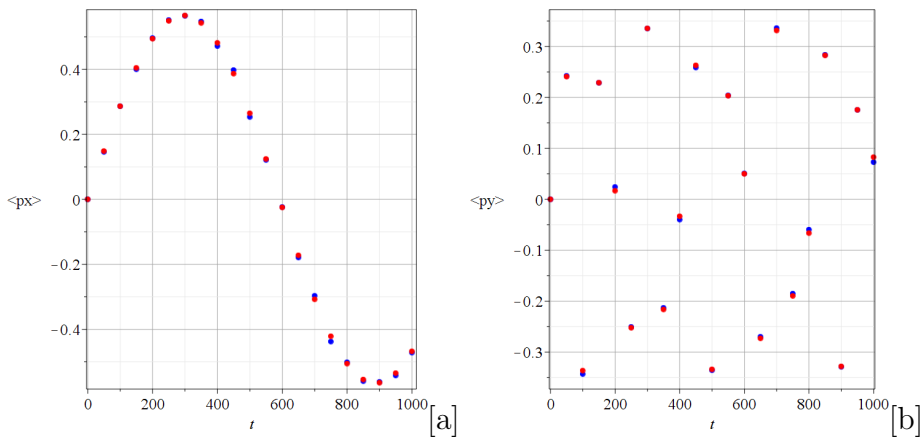


Figure 5: The average values of $\langle p_x \rangle$ (a) and $\langle p_y \rangle$ (b) as functions of time for $t \in [0, 1000]$ for every $\Delta t = 50$. The red dots correspond to the analytical values produced by Eqs. 14 and the blue dots correspond to the values produced by 5000 Bohmian particles distributed according to BR. We observe that, in both cases, the differences between the analytical and the numerical values are very small.

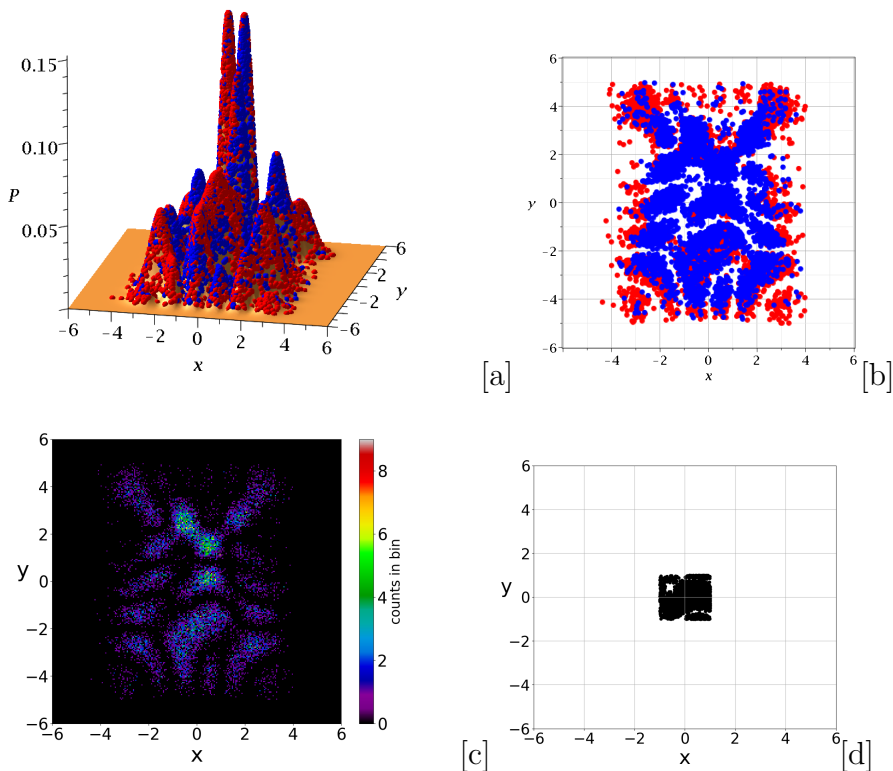


Figure 6: a,b,c: 10000 initial conditions of ordered (red) and chaotic (blue) trajectories distributed according to BR in the case of the wavefunction $\Psi = M(a\Psi_{0,2} + b\Psi_{3,4} + c\Psi_{5,7})$: a) on the surface of $P = |\Psi|^2$ and b) on the $x - y$ plane. In c) we see their colorplot at $t = 0$. d) 10000 non-Born distributed initial conditions.

Wavefunctions with many nodal points

Case 1

A wavefunction with many nodal points is

$$\Psi = M(a\Psi_{0,2} + b\Psi_{3,4} + c\Psi_{5,7}), \quad (15)$$

where the functions $\Psi_{m,n}$ are given by Eq. 4. The constants have the same values as in Section 2.

In this case the maximum m_i is 5 and the maximum n_i is 7, therefore the number of the nodal points is of order 35. An initial realization of Born's rule made out of 10000 Bohmian particles along with the surface $P_0 = |\Psi_0|^2$ is shown in Figs. 6a,b. We observe that P has many blobs that collide as they evolve in time [34]. The proportions of ordered (red) and chaotic (blue) trajectories are in this case about 50%, i.e. almost equal. The distribution of the particles at $t = 0$ is shown in the initial colorplot (Fig. 6c).

We observe that the ordered trajectories are mainly close to the tops of the two main blobs. This supports our previous results on qubit states [34, 36] made of coherent states

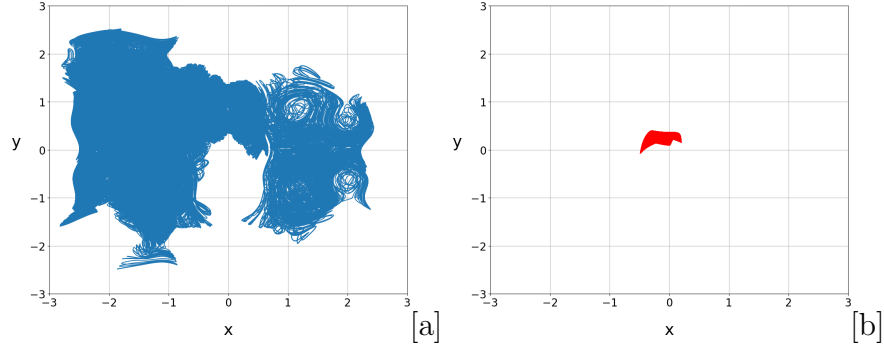


Figure 7: a,b) A chaotic ($x(0) = -0.6, y(0) = -0.01$) (a), and an ordered ($x(0) = 0.01, y(0) = 0.1$) trajectory (b), of the wavefunction $\Psi = M(a\Psi_{0,2} + b\Psi_{3,4} + c\Psi_{5,7})$.

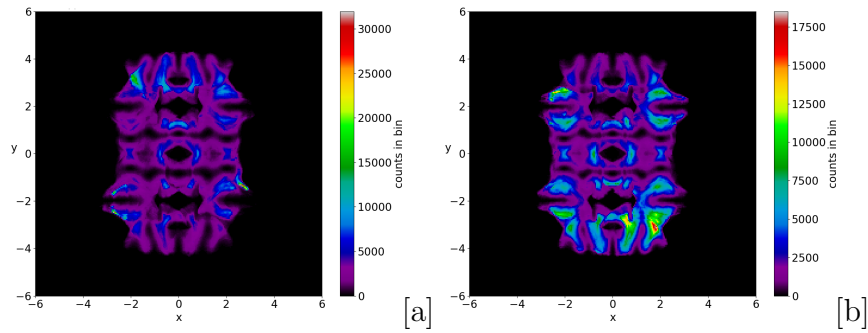


Figure 8: The colorplots of two chaotic trajectories of the wavefunction $\Psi = M(a\Psi_{0,2} + b\Psi_{3,4} + c\Psi_{5,7})$ up to $t = 2 \times 10^6$: a) $x(0) = 0.6693, y(0) = -2.4559$ b) $x(0) = -0.0631, y(0) = -1.4241$.

of the quantum harmonic oscillator, where we found that the concentration of the ordered trajectories in the Born distribution is at the top of the larger of the two blobs of $|\Psi|^2$.

The forms of the the chaotic trajectories are very irregular (Fig. 7a), while the ordered trajectories are like distorted Lissajous figures (Fig. 7b). Moreover the chaotic trajectories are ergodic as we can see in Figs. 8a,b where we show two different chaotic trajectories having very similar colorplots (cumulative distributions of points taken at every $\Delta t = 0.05$ up to $t = 2 \times 10^6$).

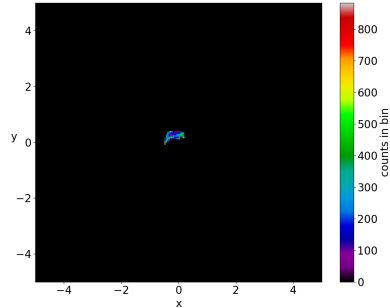


Figure 9: The colorplot of an ordered trajectory ($x(0) = 0.01, y(0) = 0.1$) up to $t = 1000$. We see that it covers a very small area of the configuration space.

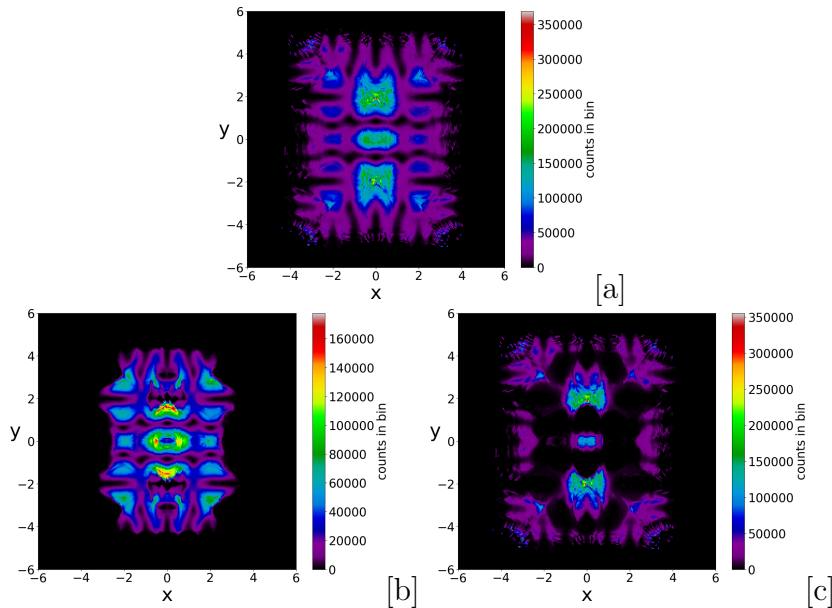


Figure 10: a) The colorplot of a realization of BR distribution consisting of 10000 particles integrated up to $t = 5000$ in the case of the wavefunction $\Psi = M(a\Psi_{0,2} + b\Psi_{3,4} + c\Psi_{5,7})$. The colorplots of the 5053 chaotic and 4947 ordered trajectories are given separately in (b) and (c).

On the other hand the colorplots of ordered trajectories cover small parts of the space (x, y) (Fig. 9). Therefore their colorplots are very different from those of the chaotic trajectories.

In Fig. 10a we show the colorplot of all the particles up to a time $t = 5000$, while the colorplots of the chaotic and of the ordered trajectories up to this time are shown in Figs. 10b,c.

We see that the colorplots Figs. 10a,b,c are quite different from each other. Therefore, if we take only chaotic (or only ordered) trajectories we will never reach the Born distribution.

As regards the average values of the observed quantities in this case we have the following: From SQM the average energy is

$$\langle E \rangle = M^2(|a|^2 E_{0,2} + |b|^2 E_{3,4} + |c|^2 E_{5,7}), \quad (16)$$

where $E_{m,n}$ are given by Eq. 6. Using the values $a = b = 1, c = \sqrt{2}/2$ and $M^2 = (a^2 + b^2 + c^2)^{-1}$ we find that $\langle E_{av} \rangle = 5.7406$. Then we calculate the average value E_{av} of $N = 10000$ Bohmian particles we find that, at $t = 0$, $E_{av} = 5.7438$. Therefore the initial deviation is of order 0.003, i.e. 0.06%.

The average values of the momentum $\langle p_x \rangle, \langle p_y \rangle$, of the angular momentum $\langle L \rangle$ and of the position $\langle x \rangle, \langle y \rangle$ are calculated analytically in the Appendix. In the present case they are all zero, i.e., $\langle p_x \rangle = \langle p_y \rangle = \langle L \rangle = \langle x \rangle = \langle y \rangle = 0$. In fact, in the Appendix we show that they are zero whenever m and n differ by more than 1 (i.e. whenever they are not adjacent integers). The corresponding mean absolute deviations from $\langle p_x \rangle, \langle p_y \rangle$ for 10000 Born distributed Bohmian particles and $t \in [0, 1000]$ are 0.009 and 0.007 respectively. Moreover, the deviations from the average angular momentum $\langle L \rangle$ and the average positions $\langle x \rangle, \langle y \rangle$ are 0.0234, 0.0122 and 0.0158 (see Table 1) and they tend to zero as time increases considerably.

On the other hand, in a case with 10000 particles distributed randomly in the square $(-1, 1) \times (-1, 1)$, i.e. away from the BR distribution (Fig. 6d), we found much larger deviations for the same time, namely about 10 times larger than the values of the Born distribution (see Table 1), which do not decrease as t increases.

Case 2

If we take

$$\Psi = M(a\Psi_{10,3} + b\Psi_{4,5} + c\Psi_{7,8}) \quad (17)$$

we have $m_i^{max} = 10, n_i^{max} = 8$, therefore the number of the nodal points is of order 80. In this case the proportion of chaotic trajectories is about 96.2% and the ordered trajectories are only 3.8%.

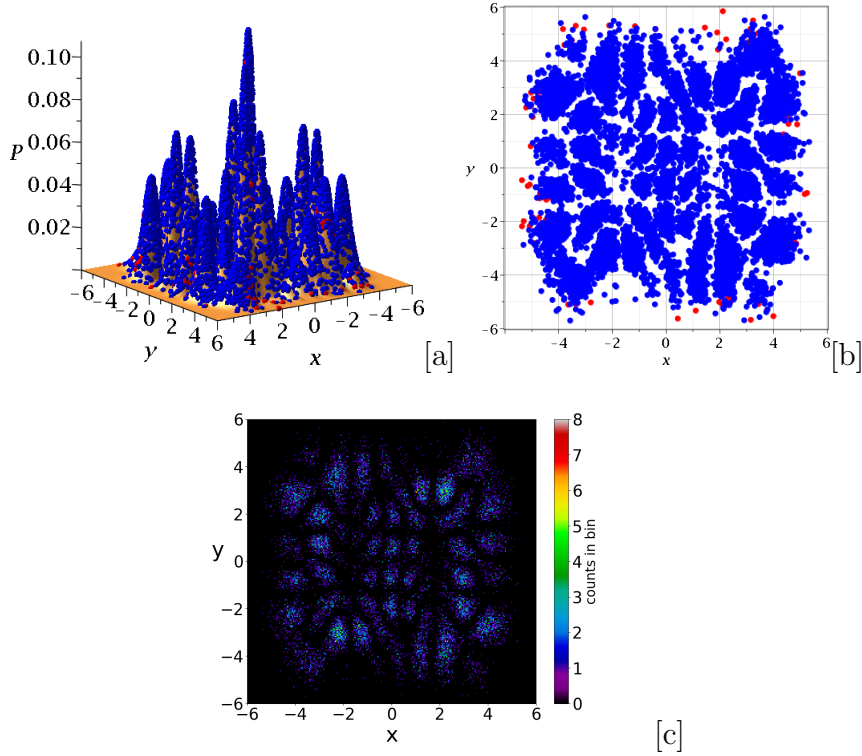


Figure 11: 10000 initial conditions of ordered (red) and chaotic (blue) trajectories distributed according to BR in the case of the wavefunction $\Psi = M(a\Psi_{10,3} + b\Psi_{4,5} + c\Psi_{7,8})$: a) on the surface of $P_0 = |\Psi_0|^2$ and b) on the $x - y$ plane ($t = 0$). c) Their colorplot at $t = 0$.

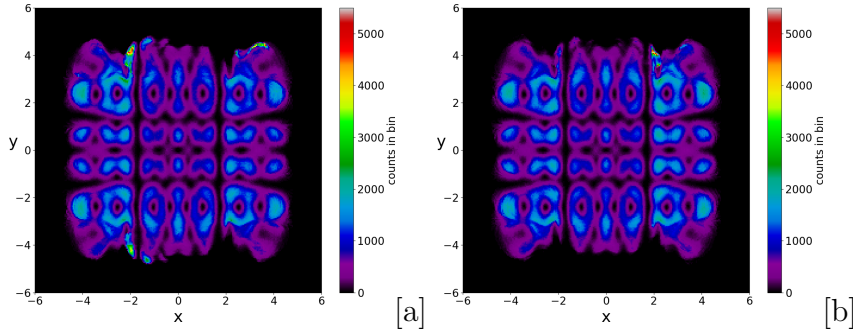


Figure 12: The colorplot of two chaotic trajectories up to $t = 10^6$ in the case $\Psi = M(a\Psi_{10,3} + b\Psi_{4,5} + c\Psi_{7,8})$: a) $x(0) = -1, y(0) = 0.7$ and b) $x(0) = -0.1, y(0) = -1.5$. They look very similar.

The initial distributions of the points according to BR is given in Fig. 11. In this case the tops of the main blobs contain mainly chaotic trajectories, which in fact are ergodic. This is shown in Fig. 12 where we compare the colorplots of two chaotic trajectories up to $t = 10^6$.

In particular, the theoretical average energy is $\langle E \rangle = M^2(a^2 E_{10,3} + b^2 E_{4,5} + |c|^2 E_{7,8})$ and this is equal to $\langle E \rangle = 11.248$. In Fig. 13 we show the numerical average at $t = 0$ as a function of the number of Bohmian particles in the Born distribution. We see that the numerical value converges to $E_{av} = 11.239$ when the number N is larger than 2000. The errors are about 0.009, i.e. of order 0.08%.

The analytical values of the average momenta $\langle p_x \rangle$ and $\langle p_y \rangle$, angular momentum $\langle L \rangle$ and position $\langle x \rangle$, $\langle y \rangle$ are zero (since the values of m and n are not different by 1, see the Appendix).

The mean absolute deviations in time are also found to be very close to zero. In particular the deviations $|\delta\langle p_x \rangle|_{av}$, $|\delta\langle p_y \rangle|_{av}$ for 10000 particles following Born's distribution and for $t \in [0, 1000]$ are 0.0082 and 0.0081. In this case the variations of a random non-Born distribution in the square $(-1, 1) \times (-1, 1)$ (taken the same as in the case 3.1) are 0.011 and 0.013, i.e. of the same order as for an initially Born distribution (see Table 1). This is due to the fact that any non-Born distribution tends to reach BR distribution in the long run when it is dominated by chaotic-ergodic trajectories.

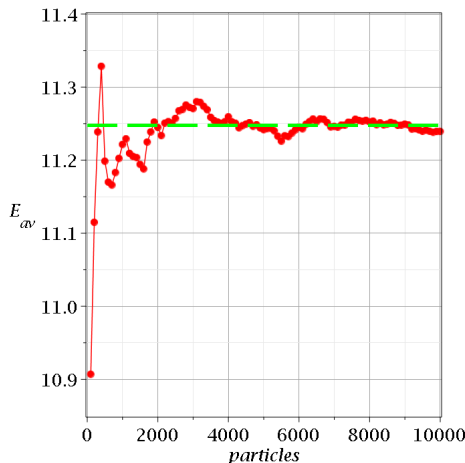


Figure 13: The average value of energy as a function of the number of trajectories in the realization of Born's rule at $t = 0$.

Conclusions

In this paper we have considered mainly distributions of particles that satisfy Born's rule $P = |\Psi|^2$. In general Born's distribution contains both chaotic and ordered trajectories. The chaotic trajectories are ergodic.

In the case of one nodal point the ordered trajectories are dominant. In the first case of many nodal points the ordered trajectories are almost equal to the chaotic trajectories, while in the second case the chaotic trajectories are dominant. In this case the Born distribution is essentially satisfied in the long run, even if the initial distribution is not Born-distributed.

However the existence of many nodal points does not necessarily imply that chaos is dominant. In fact, there are special cases of multinodal wavefunctions which are dominated by ordered trajectories. Nevertheless these cases are rather exceptional.

We calculated analytically the average values of basic quantum quantities, namely the energy $\langle E \rangle$, the momentum $\langle p_x \rangle$, $\langle p_y \rangle$, the angular momentum $\langle L \rangle$ and the position $\langle x \rangle$, $\langle y \rangle$. Their values are found analytically in the Appendix for systems of three components $\Psi = M(a\Psi_{m_1, n_1} + b\Psi_{m_2, n_2} + c\Psi_{m_3, n_3})$. We found the necessary conditions in order to have nonzero values of $\langle p_x \rangle$, $\langle p_y \rangle$, $\langle L \rangle$, $\langle x \rangle$, $\langle y \rangle$. E.g. in calculating $\langle p_x \rangle$ we must have at least two m_i indices to be different by 1 and the corresponding n_i 's equal. Similarly in calculating $\langle p_y \rangle$ we must have at least two n_i indices to be different by 1 and the corresponding m_i 's equal. In the present case of one nodal point these conditions are satisfied and $\langle p_x \rangle$, $\langle p_y \rangle$, are periodic in

Nodal points	One		Many			
Distribution	Born(3/97)	Non-Born	Born(50-50)	Non-Born	Born(96/4)	Non-Born
$ \delta\langle E\rangle _{av}$	0.0047	0.1942	0.0348	1.9518	0.0171	0.1338
$ \delta\langle p_x\rangle _{av}$	0.0053	0.2026	0.0094	0.2920	0.0082	0.0107
$ \delta\langle p_y\rangle _{av}$	0.0032	0.1525	0.0072	0.2265	0.0081	0.0130
$ \delta\langle L\rangle _{av}$	0.0082	0.3019	0.0158	0.1501	0.0416	0.1113
$ \delta\langle x\rangle _{av}$	0.0073	1.0237	0.0234	0.2177	0.0593	0.0896
$ \delta\langle y\rangle _{av}$	0.0105	0.2122	0.0122	0.1421	0.0309	0.0366

Table 1: Table of mean deviations of quantum observables between the predictions of SQM and our numerical simulations of examples of distributions of Bohmian particles for $t \in [0, 1000]$ for every $\Delta t = 50$. In parentheses we show the percentages of the chaotic and ordered trajectories in our realizations of Born distribution. We observe in the last column of the table (non-Born distribution in the case 3.2) that the mean deviations of the energy and of the angular momentum are still relatively large. They decrease for larger integration times, because in this case the distribution of particles tends to the BR distribution.

time. In general these conditions are not satisfied and the values of $\langle p_x \rangle, \langle p_y \rangle$ are zero. Similar conditions exist for the average values of the other quantum observables.

We compared the analytical values with the average values of the observed quantities by calculating a large number of trajectories with a Born initial distribution using the Bohmian equations of motion. As expected, we found a good agreement with the analytical values of SQM when the number of trajectories is sufficiently large.

However, in the cases with appreciable numbers of ordered trajectories the average numerical results do not agree with the analytical values if the initial distribution does not follow the Born rule. This is shown in Table 1 where we compare the errors of the average quantities with respect to the analytical values in the Born and the non-Born cases. The errors in the Born case are small and become even smaller when the integration time increases. On the other hand, the errors of the non-Born case are in general much larger and do not decrease in general when the time increases, except in the second case of many nodal points when the chaotic-ergodic trajectories are dominant. In this particular case any initial non-Born distribution tends practically to Born's distribution after a large time.

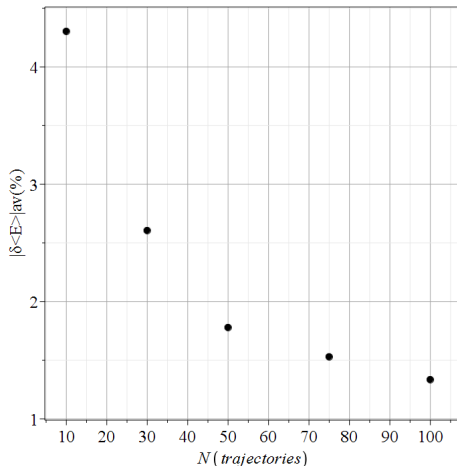


Figure 14: The mean absolute deviation (percent) between ensembles of chaotic trajectories in the case of full chaos, for $t \in [0, 10^5]$ with a time step $\Delta t = 50$ as a function of the number of the trajectories in the ensemble. Even with a few trajectories we find an average value of energy rather close to the analytical with deviations of only a few percent.

In fact, in a system where chaos is dominant one needs only a few trajectories in order to calculate with a satisfying accuracy the average values of quantum observables, but at the cost of a large integration time. This can be seen in Fig. 14 where we plot the mean absolute deviations between the theoretical and numerical average energy in the multinodal wavefunction $\Psi = M(a\Psi_{10,3} + b\Psi_{4,5} + c\Psi_{7,8})$, which is dominated by chaotic trajectories, as a function of the number of trajectories in our sample. The trajectories are integrated up to $t = 10^5$ and are sampled at every $\Delta t = 50$. We see that even with a few chaotic trajectories we find quite accurate results. E.g. with only 50 trajectories we find an average error less than 2%. These results become more accurate if we extend the integration times.

On the other hand, the ordered trajectories are mainly concentrated near the maxima of the Born distribution. They cover only a small part of the configuration space and their long time shape is not common for all of them. Therefore they cannot be simulated by the few ordered trajectories that follow Born's rule or by many ordered trajectories that are not Born-distributed.

Thus far, our series of papers on Bohmian quantum chaos has primarily focused on the generation of chaos in Bohmian trajectories and the impact of quantum entanglement [37] on the chaos-order interplay in Bohmian trajectories. Entanglement, quantified by the von Neumann entropy [38] (the quantum analogue of Shannon's entropy) was found to play a key role in the dynamical approximation of Born's rule by arbitrary initial particle distributions (for the relation between chaos and Shannon's entropy see [39]).

In systems of Bohmian qubits made out of coherent states of the harmonic oscillator we showed that chaotic trajectories increase with the degree of entanglement. In the case of maximal entanglement all the trajectories are chaotic (and ergodic) while in the zero entanglement case all trajectories are ordered.

In the present work we made a step further by trying to understand the contribution of chaotic and ordered Bohmian trajectories inside a Born distributed ensemble of Bohmian particles in the calculation of the values of the observables, something very important for the field of Bohmian chaos.

We note that, up to now, all the works on Bohmian chaos have been focused on quantum

systems that evolve according to the Schrödinger equation, i.e. closed quantum systems. This implies that the effects due to the environment, such as decoherence and dissipation, are not taken into account, something that could limit the applicability of the results obtained from these studies in more realistic, open quantum systems [40, 41]. In such systems observe a variety of environment-induced phenomena [42, 43, 44, 45, 46, 47, 48, 49, 50]. These phenomena play a key role in the field of quantum control [51, 52, 53, 54, 55].

However, while the Bohmian theory has already been applied to open quantum systems [40, 56, 57, 58], no emphasis has been given yet on the role of Bohmian chaos in the evolution of open quantum systems. In fact, the field of Bohmian chaos is still under development. And at this stage, it benefits significantly from the results found by studying closed quantum systems. The insights gained from such studies provide a fundamental understanding that can be instrumental in extending the theory to more complex, open quantum systems, where nonlinear Dynamics coexists, in general, with stochastic Dynamics.

Appendix

The theoretical average value of the $\Psi = \Psi(m_1, \sqrt{\omega_x x})$ oscillator is

$$\langle p_x \rangle = -i\hbar \int_{-\infty}^{\infty} \left(\Psi^* \frac{\partial \Psi}{\partial x} \right) dV, \quad (18)$$

since the operator \hat{p}_x is $\hat{p}_x = -i\hbar \frac{\partial}{\partial x}$. In the case of a superposition of two terms $\Psi = a\Psi(m_1, \sqrt{\omega_x x}) + b\Psi(m_2, \sqrt{\omega_x x})$ we set $\hbar = 1$ and write

$$\Psi = \frac{a\left(\frac{\omega_x}{\pi}\right)^{\frac{1}{4}} e^{-\frac{\omega_x x^2}{2}} H(m_1, \sqrt{\omega_x x}) e^{-it(m_1 + \frac{1}{2})\omega_x}}{\sqrt{2^{m_1} m_1!}} + \frac{b\left(\frac{\omega_x}{\pi}\right)^{\frac{1}{4}} e^{-\frac{\omega_x x^2}{2}} H(m_2, \sqrt{\omega_x x}) e^{-it(m_2 + \frac{1}{2})\omega_x}}{\sqrt{2^{m_2} m_2!}} \quad (19)$$

The Hermite polynomials H_m contain terms of degrees $m, m-2, \dots$, i.e. of the same parity. The conjugate wavefunction Ψ^* is found if we set $i \rightarrow -i$ in Ψ since the Hermite polynomials are real.

After some algebra we find that

$$-\left(\Psi^* \frac{\partial \Psi}{\partial x_i} \right) = \sum_i^7 F_i, \quad (20)$$

where

$$F_1 = \frac{i\omega_x^{\frac{3}{2}} H(m_1, \sqrt{\omega_x x})^2 a^2 x}{e^{\omega_x x^2} \sqrt{\pi} (a^2 + b^2) 2^{m_1} m_1!} + \frac{i\omega_x^{\frac{3}{2}} H(m_2, \sqrt{\omega_x x})^2 b^2 x}{e^{\omega_x x^2} \sqrt{\pi} (a^2 + b^2) 2^{m_2} m_2!}, \quad (21)$$

$$F_2 = \frac{i\omega_x^{\frac{3}{2}} \exp(it\omega_x m_2) H(m_2, \sqrt{\omega_x x}) H(m_1, \sqrt{\omega_x x}) 2^{-\frac{1}{2}(m_1+m_2)} abx}{e^{\omega_x x^2} \sqrt{\pi} \sqrt{m_1!} \sqrt{m_2!} (a^2 + b^2) \exp(i\omega_x m_1 t)}, \quad (22)$$

$$F_3 = \frac{i\omega_x^{\frac{3}{2}} \exp(it\omega_x m_1) H(m_2, \sqrt{\omega_x x}) H(m_1, \sqrt{\omega_x x}) 2^{-\frac{1}{2}(m_1+m_2)} abx}{e^{\omega_x x^2} \sqrt{\pi} \sqrt{m_1!} \sqrt{m_2!} (a^2 + b^2) \exp(i\omega_x m_2 t)}, \quad (23)$$

$$F_4 = -\frac{2i\omega_x H(m_1\sqrt{\omega_x x})m_1 H(m_1 - 1, \sqrt{\omega_x x})a^2}{e^{\omega_x x^2} \sqrt{\pi} m_1! (a^2 + b^2) 2^{m_1}}, \quad (24)$$

$$F_5 = -\frac{2i\omega_x H(m_2\sqrt{\omega_x x})m_2 H(m_2 - 1, \sqrt{\omega_x x})b^2}{e^{\omega_x x^2} \sqrt{\pi} m_2! (a^2 + b^2) 2^{m_2}}, \quad (25)$$

$$F_6 = -\frac{2i\omega_x H(m_2\sqrt{\omega_x x})m_1 H(m_1 - 1, \sqrt{\omega_x x})ab 2^{-\frac{1}{2}(m_1+m_2)} \exp(i\omega_x t m_2)}{e^{\omega_x x^2} \sqrt{\pi} m_2! (a^2 + b^2) 2^{m_2} \exp(i\omega_x m_1 t)}, \quad (26)$$

$$F_7 = -\frac{2i\omega_x H(m_1\sqrt{\omega_x x})m_2 H(m_2 - 1, \sqrt{\omega_x x})ab 2^{-\frac{1}{2}(m_1+m_2)} \exp(i\omega_x m_1 t)}{e^{\omega_x x^2} \sqrt{\pi} m_2! (a^2 + b^2) 2^{m_2} \exp(i\omega_x m_2 t)}. \quad (27)$$

We note that in finding the derivative of $H_m(x)$ we used the formula $H'_m(x) = 2mH_{m-1}(x)$.

The integral from $-\infty$ to ∞ of F_1 is zero since both of its terms are odd functions. Similarly both F_4 and F_5 give zero integrals since they contain different Hermite polynomials which are orthogonal. Thus the only terms that may give a nonzero contribution in $\langle p_x \rangle$ are F_2, F_3, F_6 and F_7 . The integrals of the functions F_2 and F_3 are of the form

$$\int_{-\infty}^{\infty} x e^{-x^2} H_m(x) H_n(x) dx = \pi^{\frac{1}{2}} 2^{n-1} n! \delta_{m,n-1} + \pi^{\frac{1}{2}} 2^n (n+1)! \delta_{m,n+1}, \quad (28)$$

where $\delta_{r,s}$ stands for the Kronecker symbol (see [59]). Therefore they are nonzero only if m, n differ by 1. Finally, from F_6 and F_7 we find nonzero integrals only if $m_2 = m_1 - 1$ or vice versa, i.e. the m_1 and m_2 should differ by 1 otherwise they give zero integrals.

If Ψ is the sum of 3 terms $\Psi = a\Psi_{m_1} + b\Psi_{m_2} + c\Psi_{m_3}$ then we have also terms similar to $F_1 - F_7$ between Ψ_{m_1} and Ψ_{m_3} and between Ψ_{m_2} and Ψ_{m_3} . Thus in order to have an integral different from zero we must have $|m_1 - m_2| = 1$ or $|m_1 - m_3| = 1$ or $|m_2 - m_3| = 1$. If Ψ depends both on x and y ,

$$\Psi = a\Psi_{m_1}(x)\Psi_{n_1}(y) + b\Psi_{m_2}(x)\Psi_{n_2}(y) + c\Psi_{m_3}(x)\Psi_{n_3}(y). \quad (29)$$

After the integration with respect to x we have to integrate also with respect to y , as in Eq. 8. The only integrals $\int \Psi_n(y)\Psi_{n'}(y)dy$ that are different from zero are those with $n = n'$. Therefore in a term with $|m_1 - m_2| = 1$ we must also have $n_1 = n_2$, in the term $|m_1 - m_3| = 1$ we must also have $n_1 = n_3$, and in a term $|m_2 - m_3| = 1$ we must also have $n_2 = n_3$.

Similar analytical expressions are found for $\langle p_y \rangle$ and $\langle L \rangle$. Regarding the position of the particles, the theoretical average value of x in the case of two terms gives

$$\langle x \rangle = \int_{-\infty}^{\infty} \Psi^* x \Psi dx, \quad (30)$$

where $\Psi^* x \Psi$ contains terms of the form $xH_{m_1}^2(x)$, $xH_{m_2}(x)^2$, and $xH_{m_1}(x)H_{m_2}(x)$. The integrals of the first two terms are zero. The integral of third term is different from zero only if m_1 and m_2 differ by 1. Similar results we find when Ψ contains 3 terms in x .

Then if Ψ depends also on y we must integrate also with respect to y . This integration gives zero unless $|m_1 - m_2| = 1, n_1 = n_2$ or $|m_1 - m_3| = 1, n_1 = n_3$, or $|m_2 - m_3| = 1, n_2 = n_3$.

Similarly, in calculating the theoretical average value of y we have a result different from zero only if $|n_1 - n_2| = 1$ and $m_1 = m_2$ or $|m_1 - m_3| = 1$ and $m_2 = m_3$, or $|n_2 - n_3| = 1$ and $m_2 = m_3$.

In the example of the single nodal point $\Psi = M(a\Psi_{0,0} + b\Psi_{1,0} + c\Psi_{1,1})$ we have $m_1 = 0, m_2 = 1, m_3 = 1$ and $n_1 = 0, n_2 = 0, n_3 = 1$. Therefore the x -integration for $\langle p_x \rangle$ gives two terms different from zero, those with $|m_1 - m_2| = 1$ and with $|m_1 - m_3| = 1$. The y -integration of the first term gives a non-zero term because $n_1 = n_2 = 0$ while the integration of the second term gives zero, because $n_2 \neq n_3$. The final result is given by Eq. 9. In a similar way we calculate $\langle p_y \rangle$ (Eq. 10), $\langle L \rangle$ (Eq. 11) $\langle x \rangle$ (Eq. 12) and $\langle y \rangle$ (Eq. 13).

In the example of many nodal points $\Psi = M(a\Psi_{0,2} + b\Psi_{3,4} + c\Psi_{5,7})$ (case 3.1) we have $m_1 = 0, m_2 = 3, m_3 = 5$ and $n_1 = 2, n_2 = 4, n_3 = 7$, therefore there are no terms with successive m_i, m_j and the values of $\langle p_x \rangle, \langle p_y \rangle, \langle L \rangle, \langle x \rangle$ and $\langle y \rangle$ are zero.

Similarly we have zero results in the case 3.2 when $\Psi = M(a\Psi_{10,3} + b\Psi_{4,5} + c\Psi_{7,8})$, while in the case $\Psi = M(a\Psi_{4,6} + b\Psi_{5,6} + c\Psi_{7,8})$ we have $\langle p_x \rangle$ different from zero, but $\langle p_y \rangle = 0$.

Acknowledgements

This research was conducted in the framework of the program of the RCAAM of the Academy of Athens "Study of the dynamical evolution of the entanglement and coherence in quantum systems".

References

- [1] D. Bohm, A suggested interpretation of the quantum theory in terms of "hidden" variables. i, Phys. Rev. 85 (1952) 166.
- [2] D. Bohm, A suggested interpretation of the quantum theory in terms of "hidden" variables. ii, Phys. Rev. 85 (1952) 180.
- [3] P. R. Holland, The quantum theory of motion: an account of the de Broglie-Bohm causal interpretation of quantum mechanics, Cambridge Univ. Press, 1995.
- [4] G. Bacciagaluppi, A. Valentini, Quantum theory at the crossroads: reconsidering the 1927 Solvay conference, Cambridge Univ. Press, 2009.
- [5] D. Lazarovici, M. Hubert, How quantum mechanics can consistently describe the use of itself, Sci. Rep. 9 (2019) 470.
- [6] A. Valentini, Signal-locality, uncertainty, and the subquantum h-theorem. ii, Phys. Lett. A 158 (1991) 1.
- [7] A. Valentini, Signal-locality, uncertainty, and the subquantum h-theorem. i, Phys. Lett. A 156 (1991) 5.
- [8] M. Towler, N. Russell, A. Valentini, Time scales for dynamical relaxation to the Born rule, Proc. Roy. Soc. A 468 (2011) 990.

- [9] E. Merzbacher, Quantum mechanics, John Wiley & Sons, 1998.
- [10] R. Shankar, Principles of quantum mechanics, Springer, 2012.
- [11] L. E. Ballentine, Quantum Mechanics: a Modern Development, World Scientific, 2014.
- [12] F. Haake, Quantum signatures of chaos, Springer, 1991.
- [13] H.-J. Stöckmann, Quantum Chaos: An Introduction, Cambridge Univ. Press, 1999.
- [14] S. Wimberger, Nonlinear dynamics and quantum chaos, Springer, 2014.
- [15] M. Robnik, Fundamental concepts of quantum chaos, *Europ. Phys. J. Special Top.* 225 (2016) 959.
- [16] R. H. Parmenter, R. Valentine, Deterministic chaos and the causal interpretation of quantum mechanics, *Phys. Lett. A* 201 (1995) 1.
- [17] S. Sengupta, P. Chattaraj, The quantum theory of motion and signatures of chaos in the quantum behaviour of a classically chaotic system, *Phys. Lett. A* 215 (1996) 119.
- [18] G. Iacomelli, M. Pettini, Regular and chaotic quantum motions, *Phys. Lett. A* 212 (1996) 29.
- [19] H. Frisk, Properties of the trajectories in Bohmian mechanics, *Phys. Lett. A* 227 (1997) 139.
- [20] H. Wu, D. Sprung, Quantum chaos in terms of bohm trajectories, *Phys. Lett. A* 261 (1999) 150.
- [21] A. Makowski, P. Peplowski, S. Dembiński, Chaotic causal trajectories: the role of the phase of stationary states, *Phys. Lett. A* 266 (2000) 241.
- [22] A. J. Makowski, M. Frackowiak, The simplest non-trivial model of chaotic causal dynamics, *Acta Phys. Pol. B* 32 (2001) 2831.
- [23] A. J. Makowski, Forced dynamical systems derivable from bohmian mechanics, *Acta Phys. Pol. B* 33 (2002) 583.
- [24] D. Wisniacki, F. Borondo, R. Benito, Dynamics of quantum trajectories in chaotic systems, *Europhys. Lett.* 64 (2003) 441.
- [25] P. Falsaperla, G. Fonte, On the motion of a single particle near a nodal line in the de Broglie–Bohm interpretation of quantum mechanics, *Phys. Lett. A* 316 (2003) 382.
- [26] D. A. Wisniacki, E. R. Pujals, Motion of vortices implies chaos in Bohmian mechanics, *Europhys. Lett.* 71 (2005) 159.
- [27] D. Wisniacki, E. Pujals, F. Borondo, Vortex dynamics and their interactions in quantum trajectories, *J. Phys. A* 40 (2007) 14353.
- [28] F. Borondo, A. Luque, J. Villanueva, D. A. Wisniacki, A dynamical systems approach to Bohmian trajectories in a 2d harmonic oscillator, *J. Phys. A* 42 (2009) 495103.

- [29] A. Cesa, J. Martin, W. Struyve, Chaotic bohmian trajectories for stationary states, *J. Phys. A* 49 (2016) 395301.
- [30] H. Santos Lima, M. Paixão, C. Tsallis, de Broglie-Bohm analysis of a nonlinear membrane: From quantum to classical chaos, *Chaos* 34 (2024) 023125.
- [31] C. Efthymiopoulos, C. Kalapotharakos, G. Contopoulos, Origin of chaos near critical points of quantum flow, *Phys. Rev. E* 79 (2009) 036203.
- [32] A. C. Tzemos, G. Contopoulos, Unstable points, ergodicity and born's rule in 2d bohmian systems, *Entropy* 25 (2023) 1089.
- [33] A. C. Tzemos, G. Contopoulos, Chaos and ergodicity in an entangled two-qubit Bohmian system, *Phys. Scr.* 95 (2020) 065225.
- [34] A. Tzemos, G. Contopoulos, The role of chaotic and ordered trajectories in establishing Born's rule, *Phys. Scr.* 96 (2021) 065209.
- [35] C. Efthymiopoulos, G. Contopoulos, Chaos in Bohmian quantum mechanics, *J. Phys. A* 39 (2006) 1819.
- [36] A. C. Tzemos, G. Contopoulos, Ergodicity and Born's rule in an entangled two-qubit Bohmian system, *Phys. Rev. E* 102 (2020) 042205.
- [37] R. Horodecki, P. Horodecki, M. Horodecki, K. Horodecki, Quantum entanglement, *Rev. Mod. Phys.* 81 (2009) 865.
- [38] A. C. Tzemos, G. Contopoulos, C. Efthymiopoulos, Bohmian trajectories in an entangled two-qubit system, *Phys. Scr.* 94 (2019) 105218.
- [39] F. J. Arranz, R. M. Benito, F. Borondo, Shannon entropy at avoided crossings in the quantum transition from order to chaos, *Phys. Rev. E* 99 (2019) 062209.
- [40] H.-P. Breuer, F. Petruccione, *The theory of open quantum systems*, Oxford Univ. Press, 2002.
- [41] A. Rivas, S. F. Huelga, *Open quantum systems*, Vol. 10, Springer, 2012.
- [42] N. V. Agudov, A. A. Dubkov, B. Spagnolo, Escape from a metastable state with fluctuating barrier, *Phys. A* 325 (2003) 144.
- [43] D. P. Ghikas, A. C. Tzemos, Stochastic anti-resonance in the time evolution of interacting qubits, *Int. J. Quantum Inf.* 10 (2012) 1250023.
- [44] B. Spagnolo, P. Caldara, A. La Cognata, G. Augello, D. Valenti, A. Fiasconaro, A. Dubkov, G. Falci, Relaxation phenomena in classical and quantum systems, *Acta Phys. Pol. B* 43 (2012) 1169.
- [45] A. C. Tzemos, D. P. Ghikas, Dependence of noise induced effects on state preparation in multiqubit systems, *Phys. Lett. A* 377 (2013) 2307.

- [46] L. Magazzù, A. Carollo, B. Spagnolo, D. Valenti, Quantum dissipative dynamics of a bistable system in the sub-ohmic to super-ohmic regime, *J. Stat. Mech.* 2016 (2016) 054016.
- [47] D. Valenti, A. Carollo, B. Spagnolo, Stabilizing effect of driving and dissipation on quantum metastable states, *Phys. Rev. A* 97 (2018) 042109.
- [48] G. Parisi, Nobel lecture: Multiple equilibria, *Rev. Mod. Phys.* 95 (2023) 030501.
- [49] L. Leonforte, D. Valenti, B. Spagnolo, A. Carollo, F. Ciccarello, Dressed emitters as impurities, *Nanophotonics* 10 (2021) 4251.
- [50] I. Surazhevsky, V. Demin, A. Ilyasov, A. Emelyanov, K. Nikiruy, V. Rylkov, S. Shchanikov, I. Bordanov, S. Gerasimova, D. Guseinov, et al., Noise-assisted persistence and recovery of memory state in a memristive spiking neuromorphic network, *Chaos, Solit. Fractals* 146 (2021) 110890.
- [51] S. Cong, *Control of quantum systems: theory and methods*, John Wiley & Sons, 2014.
- [52] R. Stassi, S. De Liberato, L. Garziano, B. Spagnolo, S. Savasta, Quantum control and long-range quantum correlations in dynamical casimir arrays, *Phys. Rev. A* 92 (2015) 013830.
- [53] R. Stassi, S. Savasta, L. Garziano, B. Spagnolo, F. Nori, Output field-quadrature measurements and squeezing in ultrastrong cavity-qed, *New J. Phys.* 18 (2016) 123005.
- [54] D. d'Alessandro, *Introduction to quantum control and dynamics*, CRC, 2021.
- [55] G. D. Fresco, B. Spagnolo, D. Valenti, A. Carollo, Multiparameter quantum critical metrology, *SciPost Phys.* 13 (2022) 077.
- [56] A. B. Nassar, S. Miret-Artés, *Bohmian Mechanics, open quantum systems and continuous measurements*, Springer, 2017.
- [57] X. Oriols, A. Benseny, Conditions for the classicality of the center of mass of many-particle quantum states, *New J. Phys.* 19 (6) (2017) 063031.
- [58] H. Nikolic, Quantum statistical mechanics from a Bohmian perspective, arXiv:2308.10500.
- [59] G. B. Arfken, H. J. Weber, F. E. Harris, *Mathematical methods for physicists: a comprehensive guide*, Academic press, 2011.